Fabricating Micro-Instruments in Surface-Micromachined Polycrystalline Silicon

John H. Comtois

USAF Phillips Laboratory
Space Mission Technology Division
3550 Aberdeen Avenue SE
Kirtland AFB, NM 87117

M. Adrian Michalicek

USAF Phillips Laboratory
Space Mission Technology Division
3550 Aberdeen Avenue SE
Kirtland AFB, NM 87117

Carole Craig Barron

Sandia National Laboratories
Dept. 1325/MS 1080
P.O. Box 5800
Albuquerque, NM 87185

KEYWORDS

ABSTRACT

Smaller, lighter instruments can be fabricated as Micro-Electro-Mechanical Systems (MEMS), having micron scale moving parts packaged together with associated control and measurement electronics. Batch fabrication of these devices will make economical applications such as condition-based machine maintenance and remote sensing. The choice of instrumentation is limited only by the designer's imagination. This paper presents one genre of MEMS fabrication, surface-micromachined polycrystalline silicon (polysilicon). Two currently available but slightly different polysilicon processes are presented. One is the ARPA-sponsored "Multi-User MEMS ProcesS" (MUMPS), available commercially through MCNC; the other is the Sandia National Laboratories "Sandia Ultra-planar Multi-level MEMS Technology" (SUMMiT). Example components created in both processes will be presented, with an emphasis on actuators, actuator force testing instruments, and incorporating actuators into larger instruments.

INTRODUCTION

Microelectromechanical Systems are a broad field of research of devices that range from microns to millimeters in size. Much of the technology supporting MEMS research is borrowed from the microelectronics industry; so the field takes advantage of four decades of broad, well-funded research into the properties of silicon, thin film deposition, photolithography, and related technologies. Thus MEMS research holds out the promise of batch fabrication of miniaturized machines that can be easily integrated with electronics. Micromechanics is an enabling technology like other conventional machining technologies so it does not focus on any particular application. Instead, it is being applied to problems in a wide range of fields such as biomedicine, visual displays, and aerospace sensors.

Micromechanical devices have been created with a wide variety of manufacturing processes, but nearly all of the processes depend in some way on photolithography to define small features. Regardless of how they are created, all devices are formed from two basic sets of materials, the "structural" materials that form the machinery and the "sacrificial" materials that are removed to release the machinery. The various MEMS processes differ in what these materials are and how they are deposited, patterned and

removed. Thus micromachining differs from conventional machining in which separate components are made in different fabrication processes and then joined to create the final device.

SURFACE MICROMACHINING

In surface micromachining, thin films of material are deposited by a variety of methods. A layer of photoresist is then applied and covered by a photomask which patterns the device features for that layer. The masked photoresist is exposed to light and developed, exposing the unwanted layer material which is then etched away. This photolithographic process is repeated for each layer of sacrificial and structural material until a complete micromechanical device is formed. After all layers are completed, a final release etch is performed which removes the sacrificial material from within and around the device so that the remaining structural material is free to move and perform mechanical functions.

There are many variations on this technique using different materials for the structural, sacrificial, and masking layers. Each thin film material is chosen for its mechanical, electrical, and/or chemical properties. These include polycrystalline silicon (polysilicon or "poly"), silicon nitride, silicon dioxide, metals like gold, copper or aluminum, and polyimides. Other materials have been tried, piezoelectric materials for instance, but the majority of surface micromachined devices use common microelectronic materials because of low cost and the availability of fabrication equipment.

Micromechanical devices are commercially fabricated by a number of foundries such as the Microelectronics Corporation of North Carolina (MCNC) which provides the Multi-User MEMS Process (MUMPS) [1,2]. This fabrication process has three structural layers of polysilicon with silicon dioxide as the sacrificial material. The first polysilicon layer, Poly-0, is non-releasable and is used for address electrodes and local wiring while the second and third layers, Poly-1 and Poly-2 respectively, can be released to form mechanical devices. The MUMPS process allows a layer of metal to be deposited only on the top of the Poly-2 layer. The metal is deposited as the last layer since the metal is non-refractory and the polysilicon layers are annealed at high temperatures to reduce stress. These active layers are built up over a silicon nitride layer which insulates them from the conductive silicon substrate. Figure 1 is an illustration of a simple structure fabricated in a typical surface-micromachined polysilicon process.

Some of the devices presented in this paper were fabricated in SUMMiT (Sandia Ultra-planar Multi-level MEMS Technology, through the SAMPLE (Sandia Agile MEMS Prototyping, Layout tools, and Education) service [3,4]. As in other surface-micromachining processes, MEMS devices are formed in SUMMiT by the alternate deposition of structural polysilicon layers and sacrificial oxide layers, similar to Fig. 1. The complexity of the micromachines which can be manufactured in a given process is a function of the number of independent layers of structural polysilicon the technology provides. A single level of structural material limits designers to simple sensors, since many actuators require more than one level of structural material. Geared mechanisms, for example, require two independent levels (one to form the hubs and the other the moving gears), and motorized geared mechanisms require three independent levels. Unique advantages of the SUMMiT process include one-micron feature sizes, planarization of the third poly level (Poly-3), and the ability to make flanged gear hubs and electrical contacts to the substrate.

Not shown in Fig. 1 is the topology induced in the Poly-2 by the underlying Poly-0. Thin film layers conform closely to the topology of the previously deposited and patterned layers, so they are not necessarily planar. In extreme cases the topology can trap part of a structure that was intended to move freely. Unless a device is designed to ensure the upper structural layers are flat where expected, by controlling the pattern of the layers beneath it, the induced topology can have detrimental effects on

uniformity and mechanical properties such as the effective elastic modulus. Another solution is to planarize the polysilicon layers, the approach used for Oxide-3/Poly-3 in the SUMMiT process.

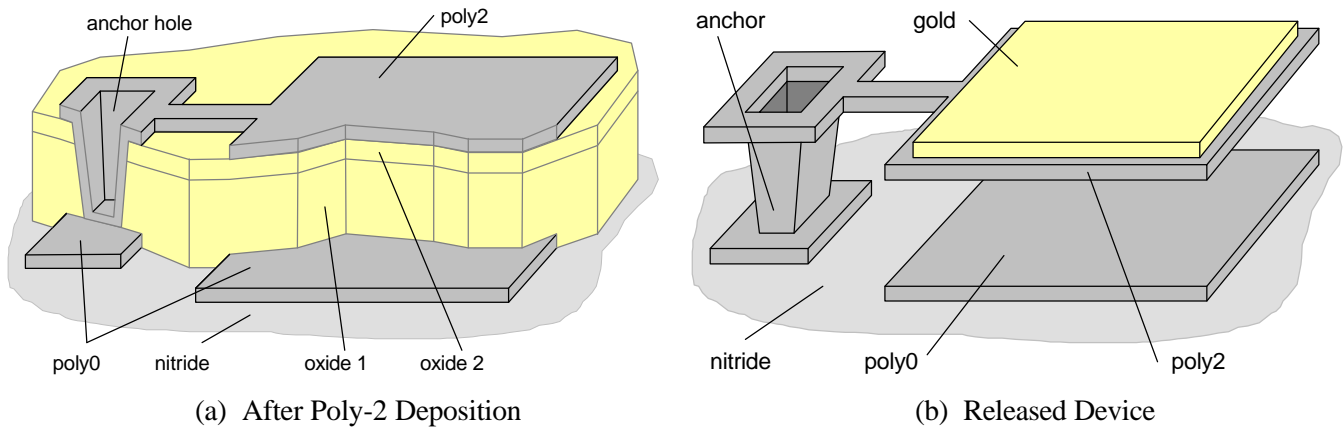(a) After Poly-2 Deposition

(b) Released Device

Figure 1. Illustration of a simple electrostatically actuated micromirror device fabricated in a surface-micromachined MEMS process [5]. For simplicity, the mirror has one only flexure and one support post. Fig. 1a shows a cross-section of this design prior to metallization. After fabrication, the sacrificial layers are etched away using hydrofluoric acid to release the structural layers forming the mechanical device. Fig. 1b shows the released micromirror after the metal has been deposited and the sacrificial material has been removed. Note that this design uses only the Poly-0 and Poly-2 structural layers.

ACTUATORS

Actuators are the features of a device or system which act on its physical surroundings mechanically, transmitting forces, motion, and energy. With actuators, a system can be built that transports, positions or otherwise moves parts of itself or parts of the environment it is operating in. Depending on its function, a system may need a variety of actuators, such as a mechanical pump for delivering drugs in an implantable system, or a mirror array modulating a light beam.

Ideally, actuators would have low power consumption, high force per unit volume, simple construction, reliable and repeatable operation, design flexibility, simple drive and control circuitry, and be compatible with the fabrication process. Because of the obvious importance of actuators to microelectromechanics, there has been research in a wide variety of actuators. The most common MEMS actuation methods include piezoelectric, electromagnetic, electrostatic, and thermal expansion.

Piezoelectric actuators, in which a material expands or contracts in response to an applied voltage, are capable of high forces and can be fabricated from thin films. This area of MEMS research draws on research in Surface Acoustic Wave (SAW) devices. However, piezoelectric actuation requires high voltage, which makes it incompatible with standard CMOS electronics, and thus harder to integrate into complete systems on a chip.
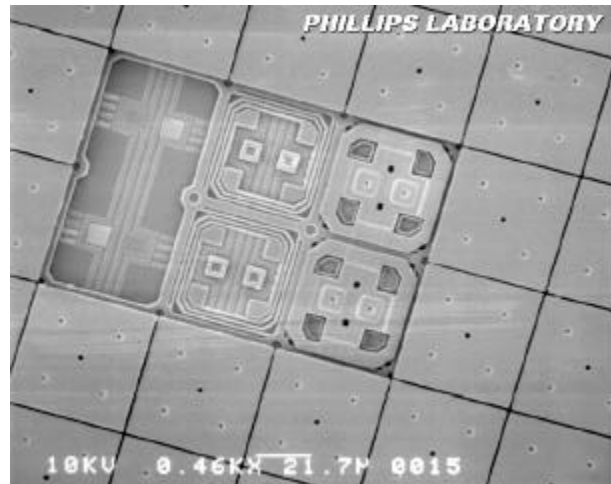
Electromagnetic actuation is common in macro-systems, in the form of electric motors and solenoids. Electromagnetic devices do not scale down well, and they are difficult to realize with surface micromachining because the planar nature of the process does not allow the creation of efficient multi-turn magnetic windings around suitable metallic cores. Thus high currents are needed to generate useful field strengths, and although external fields can be used to move magnetic microstructures, practical applications have yet to be established.

Electrostatic actuation is currently the most common MEMS actuation scheme because it does not require exotic materials or complicated fabrication. The force is generated by coulombic attraction between two structures charged to different potentials. Electrostatic actuators are capacitive structures; when a voltage is applied some feature of the actuator will move to increase the capacitance, either by closing the gap between overlapping features, or increasing the overlapping area. Electrostatic actuators are simple to fabricate in a variety of processes, they are capable of high frequency operation, and they use very little power. On the negative side, they have very low force per unit area. To achieve higher forces they require large areas, small gaps between the charged structures, or high voltages. Thus for applications requiring high forces, electrostatic actuators either use up room on the die, are expensive to fabricate, or are voltage-incompatible with standard IC electronics.

Surface-micromachined electrostatic actuators come in three varieties, lateral, vertical, and rotary. Thin film fabrication processes naturally lend themselves to creating large vertically overlapping surfaces with small gaps, thus vertical actuators can operate at lower voltages. However, this also limits the distance the actuators can move, so vertical electrostatic actuators find application mainly in optical devices where small deflections suffice. The example structure shown in Fig. 1 is a type of vertical electrostatic actuator. Micromirror devices are a common electrostatic actuator application, in which the actuation force is countered by a restoring spring force of support flexures, as shown in Fig. 2.
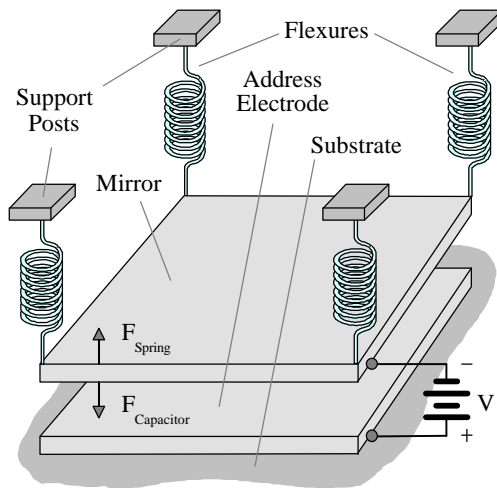
(a) Characteristic Behavior Model   (b) SEM Micrograph of SUMMiT Micromirror Details

Figure 2. Electrostatically actuated micromirrors. Fig 2a is a model for the characteristic behavior of a flexure-beam electrostatic micromirror [6,7]. Fig. 2b is a micrograph of a SUMMiT-fabricated mirror array showing the layers of the mirror design. From left to right: Poly-0 wiring, Poly-1 flexures, Poly-2 lower electrode, and the Poly-3 upper electrode and mirror surface.

Lateral electrostatic actuators take two basic forms, interdigitated combs and gap-closing structures. Gap-closing actuators are similar to vertical electrostatic actuators, but turned perpendicular to the plane of the die, so their overall deflection is still limited by the gap between the capacitor plates. Comb-style actuators allow for larger deflections, and were developed in early MEMS research [8]. A typical comb-drive actuator is shown in Fig. 3. They operate by increasing the amount of comb finger overlap, and

therefore the overall capacitance, as a voltage is applied across the combs. In this example, the center structure oscillates up and down on the page as an alternating voltage is applied to the two pairs of combs. The amount of comb finger overlap changes with motion instead of the gap between the fingers, so larger deflections are possible than with gap-closing designs.

Another common MEMS actuation scheme is based on thermal expansion, which can generate larger forces in less volume than electrostatic actuators. However, thermal actuators are much slower and use more power than electrostatic devices. The most common type of thermal actuator takes the form of a cantilever made of two layers of materials with differing thermal expansion coefficients. An embedded resistive heating element provides the heat which causes the cantilever to curl towards the side with the lower thermal expansion coefficient. Such bimorph actuators can achieve large out-of-plane deflections, have simple lithography requirements, and operate at low voltages. However, the curling motion is difficult to couple to other structures, the multi-layer design is difficult to adapt to lateral actuation, and their relatively large thermal mass results in slow actuation cycles.
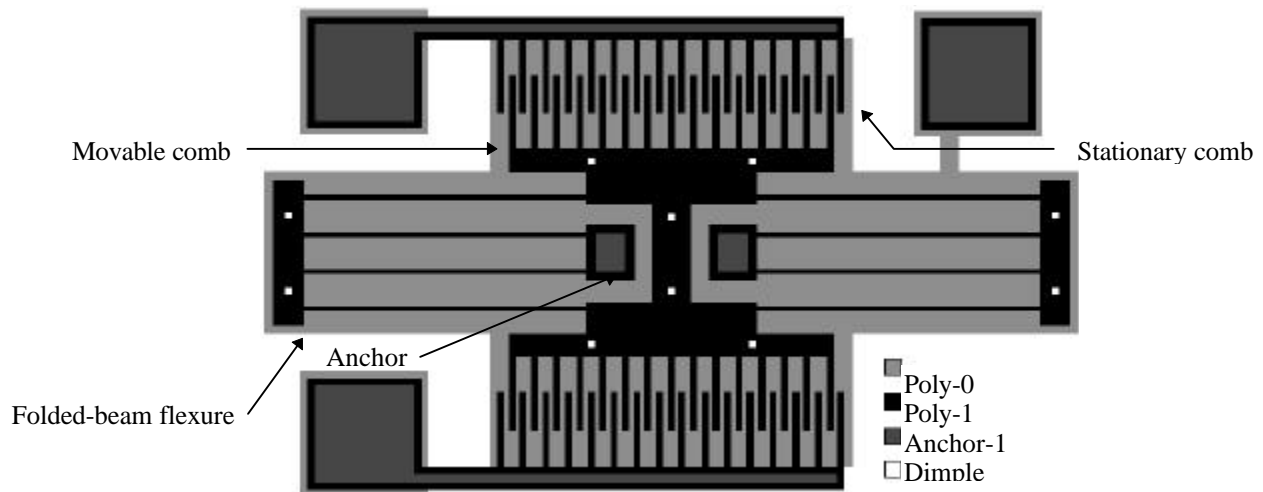

Figure 3. Layout drawing of a folded-beam electrostatic comb drive resonator. The center structure is suspended by a folded spring which is anchored and electrically connected to the Poly-0 ground plane. The spring design constrains its motion to the vertical axis. Alternating voltage applied across the two pairs of combs and the ground plane cause the center structure to oscillate. This is a test device placed on every MUMPS die by MCNC to monitor fabrication quality.

A different type of thermal actuator uses a single layer which serves as both the expansion material and the resistive heating element [9]. In this design, current passes through the device and different cross-sectional areas cause selected parts of the device to heat and expand at different rates, again resulting in a curling motion. A typical 'U' shaped lateral thermal actuator is shown in Fig. 4a. Current passes through the device from anchor to anchor, and the higher current density in the narrower 'hot' arm causes it to heat and expand more than the wider 'cold' arm, moving the tip in an arcing motion towards the cold arm side. The lower volume of heated material allows this type of actuator to operate at lower power (a few milliwatts), and higher frequencies (up to several kilohertz) than bimorph thermal actuators.

To obtain higher forces, these actuators can be connected together in arrays as shown in Fig. 4b. The actuators are electrically connected in parallel. The positive temperature coefficient of polysilicon prevents thermal runaway by diverting current to cooler actuators, resulting in even current distribution

across the array. The arrangement shown in Fig. 4b also has the advantage of converting the curling motion of the individual actuators into a purely linear motion, simplifying connection of the array to a driven structure.
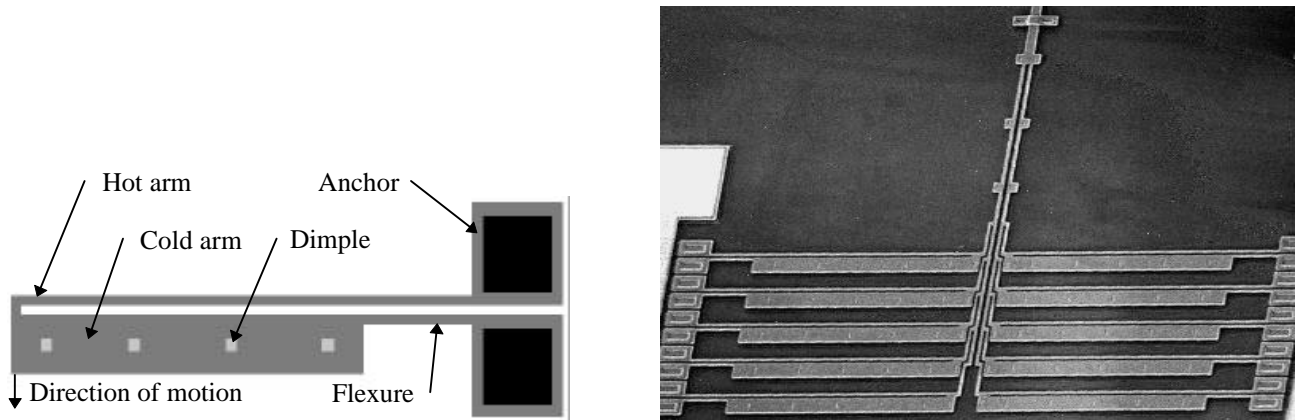
(a) Single Lateral Thermal Actuator   (b) Array of Ten Actuators

Figure 4. Fig. 4a shows the basic structure of a single layer thermal actuator[9]. Typical dimensions are: narrow 'hot' arm 2.5 μm wide, 240 μm long; wide 'cold' arm 18 μm wide, 160 μm long; flexure 2 μm wide, 50 μm long. Power required for a full 16 μm deflection is typically 12 mW at 7V. Fig. 4b shows an array of ten 240 μm long polysilicon thermal actuators connected in two groups of five by a flexural yoke. This arrangement combines forces and converts the arcing motion of the actuators into purely linear yoke motion.

INSTRUMENTATION APPLICATIONS

To extend this introduction of surface-micromachined MEMS into instrumentation applications, this section will look at examples of three types of micro-instrumentation using MEMS: instruments that determine properties of surface micromachined materials, instruments that measure characteristics of other micromechanical devices, and examples of larger instruments that could be built with surface-micromachined components. The simplest type of instrument is a single sensor such as an accelerometer, vibratory gyroscope, or gas sensor. Single sensors represent one of the broadest application areas for MEMS, with many devices being developed and several already on the market.

The mechanical properties of surface-micromachined layers are strongly dependent on the fabrication process. For example, as-deposited thin films of polysilicon can have high internal stresses which will cause released structures to curl away from the substrate. This stress can be relieved by a high temperature annealing step. The amount of residual stress is an important parameter for modeling surface-micromachined MEMS devices. Several instruments have been developed to measure this stress in-situ. In one type of strain sensor, the internal stress causes a bent beam to move an indicator, and the amount of movement is translated into a stress measurement [10]. In another approach, the stress in a released ring causes a beam along the diameter to buckle, and an array of different sized rings is used to bracket the stress value [11].

Examples of MEMS instruments used to measure the characteristics of a MEMS device are shown in Fig. 5. The test instrument in Fig. 5a is a bending-beam force tester with an integral deflection-multiplying pointer and scale. The actuators in Fig. 5b are instrumented with plain beams, with pointers

on the ends of the actuators to indicate the deflection. The devices under test are polysilicon thermal actuators. The actuators are instrumented with test beams to determine output force versus input power characteristics.

Force test beams are located on both sides of the actuators because they can be bent backwards from the initially fabricated position by controlled overheating-induced deformation of the hot arm. This deformation causes the hot arm to shorten, pulling the actuator backwards when the power is removed, as shown in Fig. 5a. The actuator shown in Fig. 5a produced a forward-bending force of 4.4 μN at an input power of 10.8 mW. This power was delivered at 2.94 V and 3.68 mA, compatible with standard CMOS electronics. The actuator deflected 16 μm at the tip when unloaded, and the 4.4 μN force was delivered at an 8 μm deflection. Force tests have also been performed on arrays of actuators [12].

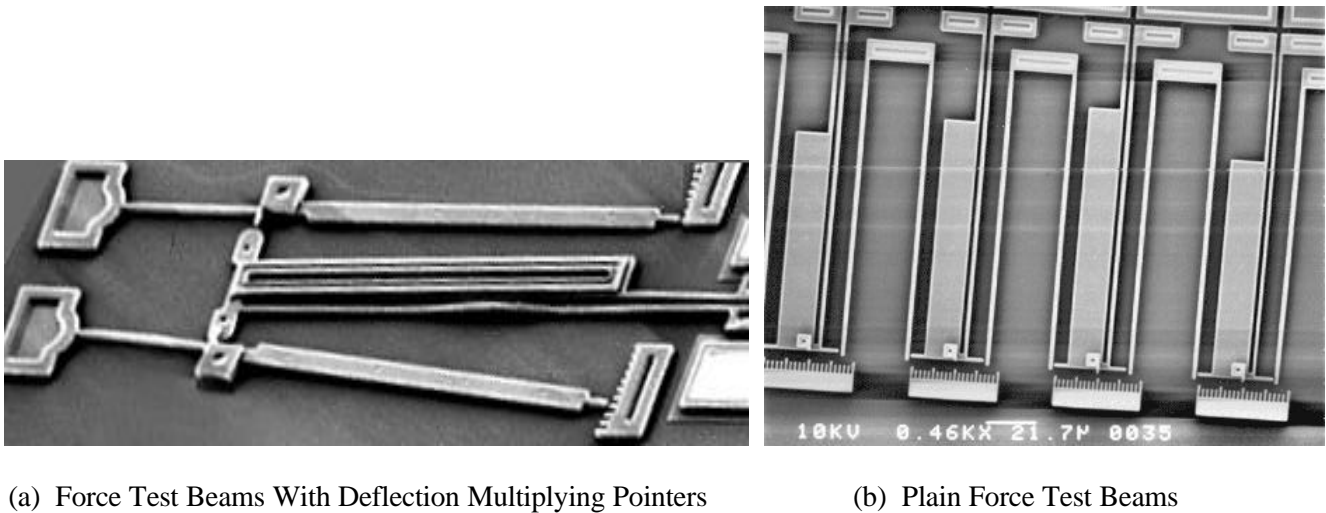(a) Force Test Beams With Deflection Multiplying Pointers   (b) Plain Force Test Beams

Figure 5.   Thermal actuators instrumented with force test beams. Fig. 5a shows a 220 μm long MUMPS-fabricated polysilicon lateral thermal actuator instrumented with force test beams. The actuator bends the test beam to deliver the force, and an extended pointer indicates deflection against a scale, which is then converted to a force measurement. This actuator is statically back-bent against the lower test beam, which is indicating a force of 15.5 μN. Fig. 5b shows SUMMiT-fabricated actuators of varying geometry instrumented with plain force test beams. The smaller feature sizes in this process allow usable deflections to be indicated directly by a pointer on the actuator tip.

Note that the deflection read off the scale in Fig. 5a is not a simple length-ratio multiplication of the deflection at the point of force application, since the beam is curved up to that point and straight from there to the scale, as shown in Fig. 6. Equation (1) shows the deflection versus force for this geometry.

$$F = y' \left[\frac{Ehw^3}{\left(4L^3 + 6L^2 L'\right)} \right]$$

(1)

This relationship is based on Hooke's law, and the inertia of a beam with rectangular cross-section [13]. The terms are those illustrated in Fig. 6, plus the force F, Young's modulus E, the width of the beam w, and the height of the beam h. In practice, the factor in square brackets is pre-calculated from known

geometries and Young's modulus, then used to convert the observed $y¢$ to the force F by simple multiplication.
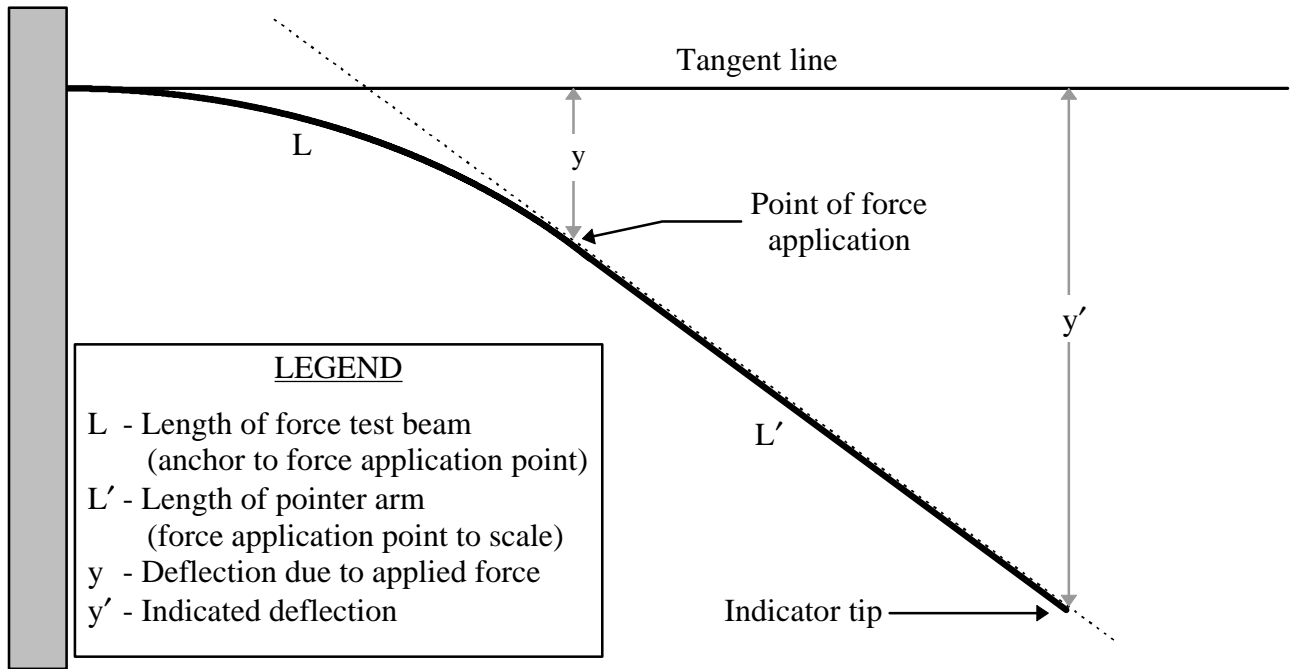

Figure 6. Geometry of a bent force testing beam. The pointer section of the beam extends past the point of force application to multiply the deflection. The multiplied deflection is indicated on a scale as seen in Fig. 5a.

MEMS devices can also be used to build up larger instruments. Fig. 7 shows a 185 x 200 μm optical grating having 2 μm lines and 2 μm spaces which is rotated using the thermal actuator arrays described above [14]. This device can in turn be made part of a larger instrument such as a spectrometer or a monochromator. A example spectrometer, shown in Fig. 8 was designed as a mechanical demonstration system to show a rotationally positioned device 'in use'. A spectrometer uses a rotating grating to diffract different wavelengths from the source to the output aperture. A flip-up, rotating grating is the key component in this system. Other components include angled mirrors to couple light perpendicularly on and off the die, and a polysilicon filament infrared (IR) light source. The mirrors, grating, and IR source are manually flipped up on hinges to create the final 3-D instrument.

Another complex instrument is the interferometer shown partially assembled in Fig. 9. This device modulates an optical signal [15]. The signal comes into the interferometer from an optical fiber or is coupled in with fold-up mirrors, similar to the spectrometer above. A grating is used to split the incoming signal, and the energy diffracted into the ±1 orders is fed down two optical paths. One path has a fixed mirror and the other has a mirror that can be moved with thermal actuators. There is a hinged plate to block the zero order energy passing straight through the grating. A second grating recombines the light from the two paths which now interfere constructively or destructively depending on the position of the movable mirror. In Fig. 9, the fixed mirror has not been raised so the rest of the interferometer components can be seen. The input grating is attached with a tether to the blocking plate so both can be raised at the same time. The moving mirror is attached to a pair of thermal actuators by tethers on either

side. One of these tethers can just be seen running off at the upper right corner of the picture. The overall size of the interferometer is 172 x 400 μm.
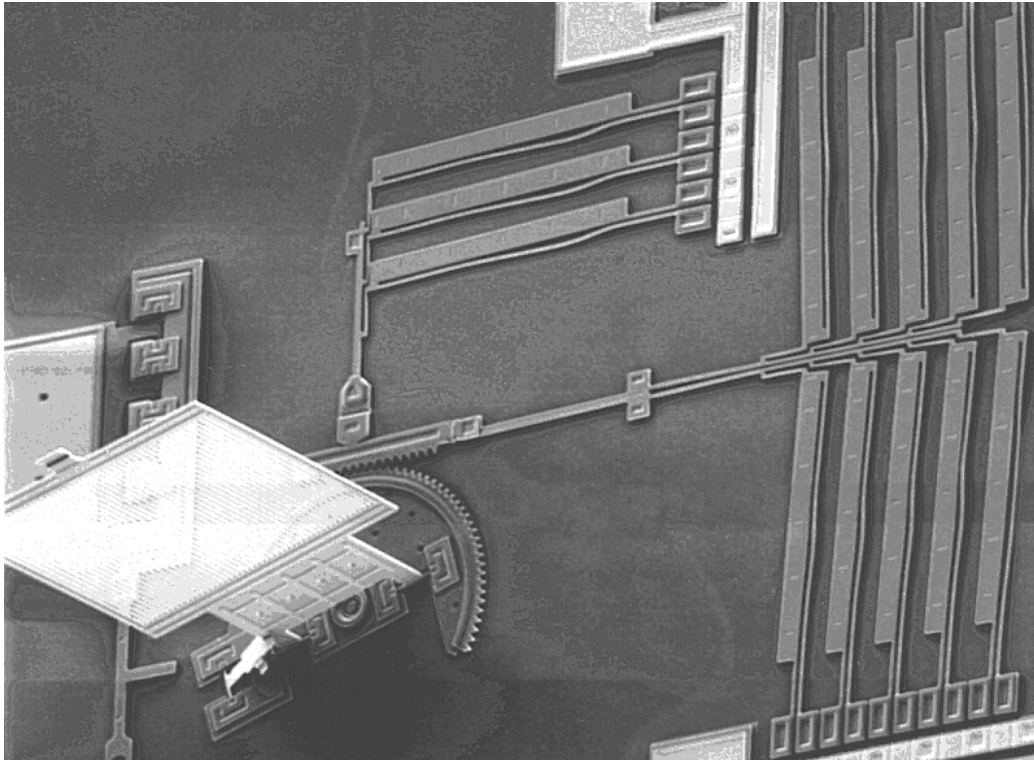

Figure 7. A vertical, rotating 185 x 200 μm optical grating having 2 μm lines and 2 μm spaces. The grating is rotated by a stepper motor based on thermal actuator arrays. This grating is part of the microspectrometer shown in Fig. 8; one of the fold-up hinged mirrors can be seen at the extreme left.
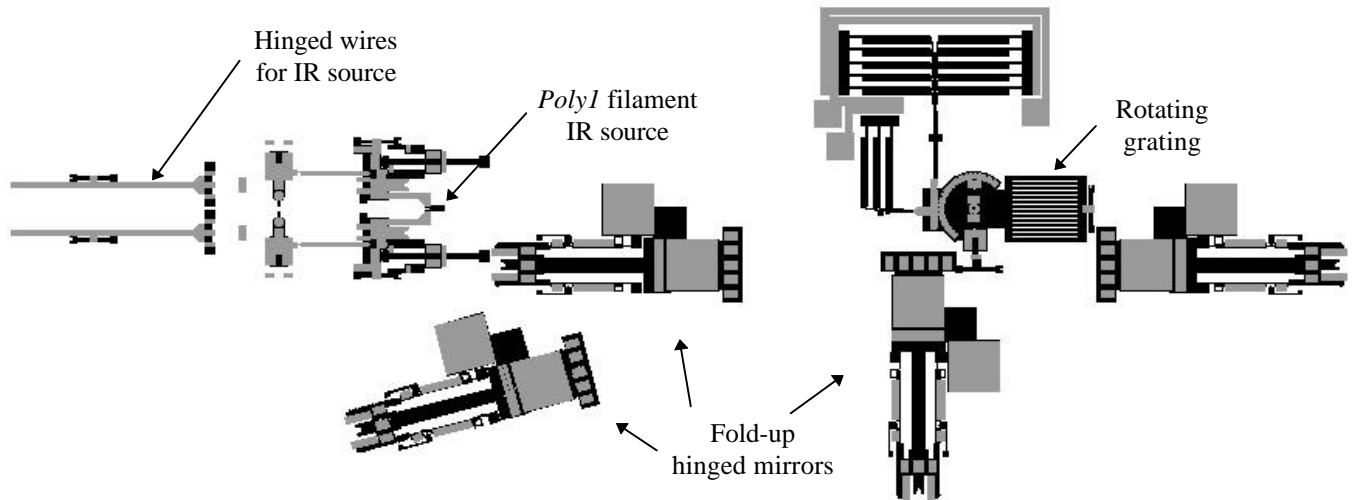
Figure 8. Infrared microspectrometer designed in the MUMPS process to demonstrate an application of a rotationally positioned optical component. Slide-up mirrors make optical connections perpendicular to the die surface. Mirrors are set at 0°, 15° and 90° to the grating and are folded up to a 45° angle for operation. A hinged frame with a Poly-1 filament acts as an infrared light source. The frame is rotated perpendicular to the substrate, and flexible wires carry current to the filament.
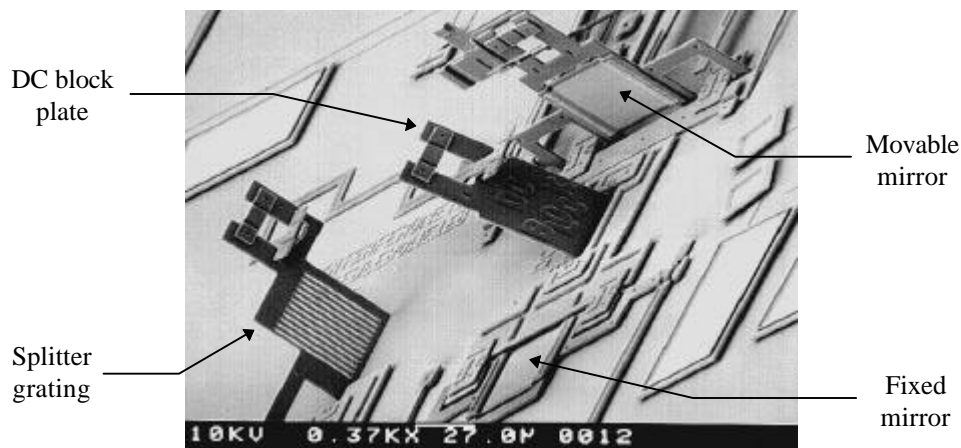

Figure 9. Partially assembled microinterferometer [15]. The grating on the left is the beam splitter. The plate marked 'DC BLOCK' blocks the zero order energy coming straight through the grating. The raised mirror behind the block is attached to two thermal actuators, not shown. The fixed mirror is not raised, and the second grating is not visible, off the right side. All optical components are roughly 50 μm square.

ACKNOWLEDGEMENT

REFERENCES

1.   D. Koester, R. Mahedevan, and K. Marcus, *Multi-User MEMS Processes (MUMPS) Introduction and Design Rules*, revision 3, Oct 1994, MCNC MEMS Technology Applications Center, 3021 Cornwallis Road, RTP, NC, 27709.

2.   MCNC Home Page: http://www.mcnc.org

3.   E. J. Garcia and J. J. Sniegowski, "Surface Micromachined Microengine", Sensors and Actuators A 48 (1995) 203-214.

4.   Sandia National Laboratories MEMS Home Page: http://www.mdl.sandia.gov/Micromachine

5.   J. Comtois, V. Bright, S. Gustafson and M. Michalicek, "Implementation of hexagonal micromirror arrays as phase-mostly spatial light modulators," Proc. SPIE Microelectronic Structures and Microelectromechanical Devices for Optical Processing and Multimedia Applications, Vol. 2641, pp. 76-87, 23-24 October 1995.

6.   M. A. Michalicek, D. E. Sene, and V. M. Bright, "Advanced modeling of micromirror devices," Proc. Advanced Micro/Nanotechnology for Space Applications, pp. 214-229, 30 October 1995.

7.   M. A. Michalicek, V. M. Bright, and J. H. Comtois, "Design, fabrication, modeling, and testing of a surface-micromachined micromirror device," Proc. ASME, DSC vol. 57-2, pp 981-988, 1995.

8.   W. Tang, T. Nguyen and R. Howe, "Laterally driven polysilicon resonant microstructures," Sensors and Actuators, vol. 20, pp. 25-32, 1989.

9.   J. H. Comtois, V. M. Bright, and M. W. Phipps, "Thermal microactuators for surface-micromachining processes," Proc. SPIE, vol. 2642, 1995, pp. 10-21.

10. Y. Gianchandani and K. Najafi, "A compact strain sensor with a bent beam deformation multiplier and a complementary motion vernier," Solid State Sensors and Actuators Workshop, Hilton Head, SC, 1994, pp. 116-118.

11. H. Guckel, D. Burns, C. Rutigliano, E. Lovell, and B. Choi, "Diagnostic microstructures for the in situ measurement of the mechanical properties of thin films," Journal of Micromechanics and Microengineering, Vol. 2, 1992, pp. 86-95.

12. J. R. Reid, V. M. Bright, and J. H. Comtois, "Force measurements of polysilicon thermal micro-actuators," Proc. SPIE: Micromachined Devices and Components II, vol. 2882, pp. 296-306, 14-15 Oct. 1996.

13. A. Simon and D. Ross, Principles of Statics and Strength of Materials, Wm. C. Brown Company, Dubuque, Iowa, 1983.

14. J. H. Comtois and V. M. Bright, "Surface Micromachined Polysilicon Thermal Actuator Arrays and Applications", Solid State Sensors and Actuators Workshop, Hilton Head, SC, 1996, pp. 174-177.

15. D. Sene, "Design, fabrication and characterization of micro-opto-electro-mechanical systems," Master's thesis, Air Force Institute of Technology, Wright-Patterson AFB, Ohio, AFIT/GEO/ENP/95D-03, Dec 1995, available through DTIC.